Journal of
Ceramic Science
and Technology

J. Ceram. Sci. Technol., **16** [3] 135-140 (2025)
DOI: 10.4416/JCST2024-00017
available online at: http://www.ceramic-science.com

The Influence of Titania, Carbon Black and Graphite on the Spinel Formation in a Magnesia Alumina Castable

J. Angelkort*[1], L. Himmel[1], Y. Lakotta-Weinhold[1], A. Reichert[1], M. Mix[1]

[1]Intocast AG, Westpreussenstrasse 30, 47809 Krefeld, Germany

received September 7, 2024; received in revised form February 27, 2025; accepted April 30, 2025

Abstract

In this work, we studied the effect of small additions of titania and three carbon sources on the spinelization of magnesia alumina castables. Compared to additive-free reference samples, titania-containing magnesia alumina castables were found to exhibit improved sinterability and higher cold crushing strength after firing. In parallel, significantly higher amounts of spinel formed during heat treatment when titania had been added to the castable.

For the carbon-containing samples, the grain size of the carbon source proved to be an important parameter controlling the influence on spinelization. While the addition of carbon black (particle size $d_{90} < 1$ µm) clearly facilitated the spinel formation at a temperature of 1 200 °C, the influence of small-flake graphite (particle size $d_{90} \sim 75$ µm) was less pronounced. The use of large-flake graphite (particle size $d_{90} \sim 180$ µm) ultimately even hampered the spinelization reaction at this temperature. This latter effect is attributed to the presence of large graphite flakes which presumably inhibit the chemical reaction in the sample by blocking the direct contact between alumina and magnesia grains.

Keywords: Spinel formation, castable, titania addition, carbon addition, sintering.

I. Introduction

Due to their high-temperature resistance and low chemical reactivity, spinel-forming and spinel-containing castables are widely employed as lining materials in the steel industry. In spinel-forming castables, magnesia and alumina react to spinel upon heating, embedding larger aggregates, like e.g. tabular alumina grains, in a fine-grained matrix of spinel. Several additives are known to influence the spinel formation [1–5]. Volume expansion accompanying the spinel formation is partly driven by density differences of the phases involved in the phase formation, i.e. magnesia, alumina and spinel. However, also other effects, like e.g. the Kirkendall effect, which is caused by different diffusion coefficients of the pertaining chemical elements, impact on the volume increase as well [6,7].

One important process mostly associated with a decrease of the sample volume at high temperatures is grain sintering. Often the sintering process is facilitated if a small amount of a liquid phase forms allowing a rearrangement of the grains and a reduction of stress in the refractory material [8]. Recently, it has been shown that additions of titania (TiO_2) increase the amount of liquid phase developing in magnesia-based castables during heating and impact on the mechanical strength of the fired product [4]. As suggested by a previous study, also for spinel-forming magnesia alumina castables the mechanical strength can be substantially increased if titania is added to the precursor material [5]. In this work, we wanted to scrutinize how the mechanical strength of the magnesia alumina castable responds to a variation of the titania content in the castable and what is the effect of the titania additions on the amount of the *in-situ*-formed spinel.

Probably, the main effect of the titania addition in spinel-forming castables is driven by improved sinterability. However, also the incorporation of titanium ions in the spinel structure may influence important key properties of the castable. In magnesium titanate karrooite ($MgTi_2O_5$) for example, the Mg-O bond is significantly weaker than the Ti-O bond [9], and cation exchanges in the crystal structure may effect profound changes in the phase stability of the compound [9,10].

Although partly quite different in their chemical behavior, the members of both the titanium group (group 4 in the periodic table of the chemical elements) and the carbon group (group 14 in the periodic table) possess four valence electrons and adopt the oxidation state +4 in oxidizing environments. Because carbon tends to form covalent bonds, it seems probable that only small amounts of carbon might be incorporated in spinel. On the other hand, carbon additions in spinel-forming refractories have been reported to influence spinelization and to increase the mechanical strength of fired castables [11,12]. As spectroscopic investigations indicate, carbon does enter the spinel structure, at least temporarily, at elevated temperatures via lattice defects [13]. It should be stressed, however, that carbon additions probably influence the spinel formation also by other mechanisms, involving e.g. gas phase reactions and vapor deposition processes. Although still uncertain by which mechanism carbon acts on the spinelization, we

* Corresponding author: Joachim.Angelkort@intocast.de

found it appealing to investigate the effect of selected carbon sources on the properties of a spinel-forming castable and its phase composition.

II. Experimental Section

The effect of titania, carbon black and graphite on spinel formation was investigated by examining the influence of these additions on the properties of lab-produced sample cylinders. The sample cylinders had diameters of 50 mm and measured 50 mm in height. They were cast from aqueous model masses that had a water content of 12 wt% and prepared from eight different dry mixtures (Table 1). The dry mixtures weighed ~2 kg and contained fine-grained alumina (Al_2O_3), magnesia (MgO) and a small amount of one of the four additives (Tables 1 and 2). Throughout this paper, dry-mixtures and castables are referred to with labels indicating both the type of additive added in the sample and the quantity in which the additive was added (Table 1).

Table 1: Relative amounts of raw materials combined to dry mixtures, values in wt%.

Sample	Magnesia	Alumina	Titania	Carbon black	Graphite, small grains	Graphite, large grains
X	28	72	-	-	-	-
T1	28	71	1	-	-	-
T2	27	71	2	-	-	-
T3	27	70	3	-	-	-
T5	26	69	5	-	-	-
CB3	27	70	-	3	-	-
GS3	27	70	-	-	3	-
GL3	27	70	-	-	-	3

In the dry mixtures, equal amounts of reactive and tabular alumina were combined to balance the water demand and the flowability of the masses. From each mass, three sample cylinders were cast. After demolding, the cylinders were dried for one day at room temperature and 110 °C, subsequently. The dried cylinders were either used for dilatometry measurements or fired for 5 hours at 1 200 or 1 500 °C. The dilatometry measurements were carried out as a refractoriness under load (RUL) experiment in air employing a Netzsch RUL/CIC 421 instrument. During the measurements, the sample temperature was increased at a heating rate of 5 K/min while a sample load of 0.02 MPa was applied.

The mechanical strength of the heat-treated samples was probed by measuring the cold crushing strengths (CCS) of the cylinders using a standard testing machine supplied by Form+Test that determines CCS values with standard uncertainties smaller than 0.3 %. To inspect the microstructures of the samples, a Hitachi TM3000 scanning electron microscope was used. Powder X-ray diffraction (XRD) patterns were recorded for a scattering angle 2θ ranging from 4 to 70 deg using a PANalytical X'Pert[3] diffractometer equipped with a copper X-ray tube. The measured XRD patterns were used to perform qualitative and quantitative phase analysis employing the computer program HighScore from PANalytical and database entries from the Crystallography Open Database [14].

III. Results and Discussion

In dilatometric measurements, the linear thermal expansions of sample cylinders were measured as a response to increasing the temperature from room temperature to 1 650 °C (Fig. 1). Plots of the measured data show that curves of titania-containing samples deviate characteristically from the curve found for the titania-free reference sample X. The higher the amount of titania in the sample, the more the profile maximum seems to be shifted to lower temperatures, with the shape of the curve around the maximum becoming more asymmetric (Fig. 1, upper section). Concomitantly, the thermal expansions determined for the temperature T = 1 650 °C decrease with the titania content in the samples. Castables containing titania in amounts of 3 or 5 wt% even seem to shrink during the dilatometric measurement if just the initial and final cylinder heights are compared. This behavior might be regarded as an indication of a lowering of the high temperature resistance of the castable induced by the TiO_2 addition. We observed, however, for some of our samples, which were re-used after completion of the RUL measurement for another heating cycle in a second RUL measurement, that TiO_2-containing castables do not shrink substantially more than a TiO_2-free sample during a second heating cycle. The presence of small amounts of TiO_2 seems therefore rather to promote the densification of the castable during a first heating event and not to induce a permanent decrease in the high-temperature resistance of the castable.

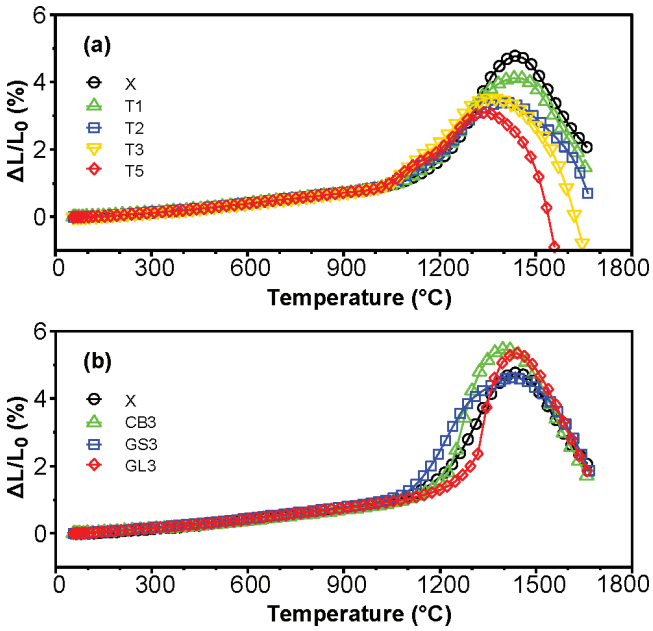

Fig. 1: Dilatometric plots measured on different samples. (a) plots compiled for samples containing 0 to 5 wt% TiO_2, (b) compilation for carbon-added samples. Samples labeled accordingly to Table 1.

The influence of titania additions on the sintering behavior of the castables can also be followed based on a comparison of the volume changes ΔV (Tables 3 and 4), calculated for the sample cylinders from heights and diameters of the samples measured before and after the heat-treatment. For castables fired at 1 500 °C, the titania additions are associated with a quantity-dependent decrease of the ΔV values. In contrast to that, castables fired at 1 200 °C show an increase of the expansion ΔV for titania additions up to 2 wt%. Higher titania additions (like in samples T3 and T5) result, however, in a decrease of the volume expansion. For castables fired at 1 200 °C, the titania additions seem therefore to induce two competing effects on the sample volume. On one hand, the titania addition impacts on the sample volume by improving the grain sintering. On the other hand, the titania addition also influences the spinel formation rate. As the spinel formation is associated with an increase in the sample volume, for certain temperatures and small amounts of added titania, this expansion might offset the decrease in the sample volume caused by the grain sintering.

The results of the quantitative phase analyses indicate that the phase amount of spinel in the heat-treated castables increases with the amount of added titania (Tables 5 and 6). In castables heat-treated at 1 200 °C, the spinel content rises from 46.9 wt% to 61.3 wt% by increasing the titania content from 0 wt% (sample X) to 5 wt% (sample T5). In the samples heat-treated at 1 500 °C, the effect of the titania addition on the spinel formation is less pronounced since all samples display spinel contents higher than 90 wt%. Nonetheless, the samples heat-treated at 1 500 °C also formed higher amounts of spinel when the precursor material contained titania additions (Table 6).

The fired castables contained a small amount of Ca- and SiO_2-containing phases (Tables 5 and 6), which probably developed as a result of reactions between impurities of the raw materials (Table 2) with the major constituents of the samples. As the titania used for our experiments contained a significant amount of SiO_2, it might even be that the silica content exerted a positive effect on the spinel formation process as well. In a previous study, it was found, however, that 1 wt% SiO_2 caused a much smaller effect on the spinelization than 1 wt% TiO_2 [5].

In the XRD patterns measured for samples T3 and T5, a set of peaks was identified as Bragg reflections of a phase possessing the chemical formula $MgAl_2Ti_3O_{10}$ [15,16]. To estimate the amount of the $MgAl_2Ti_3O_{10}$ phase in the samples, a structure model of karrooite – the Mg-rich analog of the iron titanate ferropseudobrookite – was used in the quantitative phase analyses [9,17]. This approach was chosen because no structural information for the $MgAl_2Ti_3O_{10}$ phase was found in the COD data base. As differences in the two structures are assumed to arise mainly from a distribution of Al atoms on atomic sites solely occupied by Mg and Ti atoms in karrooite, the error in the phase analysis calculations caused by using a structure model of karrooite (COD code 9002015) instead of $MgAl_2Ti_3O_{10}$ was anticipated to be low. In fact, the phase analysis calculations for samples T3 and T5 converged with acceptable R values (R_p ~ 8 %). Based on the calculations, the karrooite content in the two samples was estimated to be ~ 1 and ~ 3 wt%, respectively.

Table 2: Typical chemical composition and grain size (d_{90}) of different raw materials.

Reactive alumina	
99.7 % Al_2O_3, 0.3 % others	7 μm
Tabular alumina	
99.5 % Al_2O_3, 0.5 % others	150 μm
Magnesium oxide	
97.2 % MgO, 2.1 % CaO, 0.25 % SiO_2, 0.25 % Fe_2O_3, 0.3% others	50 μm
Titanium oxide	
80 – 90 % TiO_2, SiO_2 < 9 %, Fe_2O_3 < 2 %, Al_2O_3 < 3 %	~ 250 μm
Carbon black	
C content > 99 %	< 100 nm
Graphite, amorphous, small flakes	
C content > 80 %, ~ 8 % SiO_2, ~ 4 % Al_2O_3, ~2 % CaO	< 75 μm
Graphite, crystalline, large flakes	
C content > 98 %	< 180 μm

As the cold crushing strengths of the heat-treated castables show a clear correlation with the titania content (Tables 3 and 4), the increase of the titania content from 0 to 5 wt% seems to stimulate grain sintering. SEM micrographs corroborate a gradual increase of both the average grain size of the *in-situ*-formed spinel and the average pore size with an increasing amount of titania in the castables (Fig. 2). While the average grain size of spinel can be estimated to be ~ 1 μm after heat-treating the reference sample X at 1 500 °C, the grain size is ~ 5 – 10 μm in the heat-treated sample T5. The grain coarsening is associated with Ostwald ripening, favoring growth of larger grains at the expense of the smaller ones. The occurrence of the larger grains in the titania-rich samples demonstrates, in parallel, the efficiency of titania as a sintering aid. To assess the effect of TiO_2 additions on the mechanical strength of castables heated to temperatures corresponding to the service temperatures of linings in the steel industry, however, further studies need to be undertaken determining e.g. the hot modulus of rupture of castables containing different TiO_2 contents.

In contrast to the improved sintering for titania-containing samples, additions of carbon black or graphite were not found to significantly increase the mechanical strength of the castables. Although the addition of small-flake graphite results in a small increase of the cold crushing strength of the fired castables GS3, both the addition of carbon black and large-flake graphite causes even a drastic decrease in the mechanical strength compared to the reference sample X. As the small-flake graphite contains a quite large amount of silica and other impurities (Table 2), the

higher CCS values measured for sample GS3 could possibly result from the occurrence of a finely dispersed silica-rich melt facilitating the grain sintering at high temperatures.

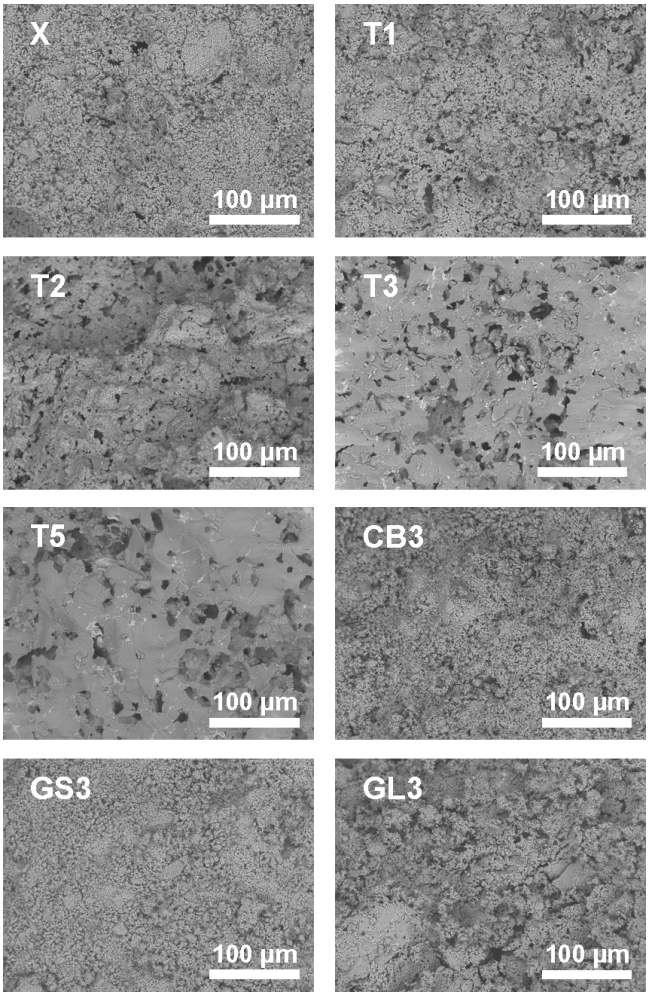

Fig. 2: SEM micrographs of samples heat-treated at 1 500 °C. Samples labeled as in Fig. 1.

After heat-treatment at 1 200 °C, the amount of spinel is slightly larger in sample CB3 (51.4 wt%) and GS3 (48.0 wt%) than in the reference sample X (46.9 wt%). However, the amount of spinel is found to be significantly lower in sample GL3 (38.4 wt%). This observation might be interpreted in terms of the presence of larger graphite flakes in GL3, possibly preventing the progress of the spinel formation by embedding carbon interlayers between magnesia and alumina grains.

After the heat-treatment at 1 500 °C, the cylinder of sample CB3 showed several cracks. Maybe these developed as consequence of a rather rapid release of carbon dioxide affected by a fast oxidation of the nano-sized carbon particles during heating. In this context, it might be interesting to compare the plots of the dilatometric measurements (Fig. 1). Up to a temperature of ~ 1 200 °C, reference sample X and sample CB3 follow the same trend in the temperature-dependent expansion. In the temperature interval between ~ 1 200 and ~ 1 250 °C, however, the measurement of sample CB3 shows a significantly steeper slope than the plot measured for sample X. The additional expansion of sample CB3 in this temperature range might be associated with the burning of the carbon source. The steeper slope of the expansion in this temperature interval probably results in a higher stress, possibly accounting for the crack formation in sample CB3. Furthermore, the dilatometric plot of sample GL3 shows the deviation from linearity to set in at a higher temperature than reference sample X, indicating that the spinelization process is hindered by the presence of large-flake graphite.

Table 3: Mass and volume changes caused by heat-treating samples at 1 200 °C together with measured cold crushing strengths of the fired castables.

	Δm [%]	ΔV [%]	CCS [MPa]
X	-1.2	13.3	5.5
T1	-1.5	13.9	6.6
T2	-1.8	16.4	7.4
T3	-1.4	12.5	8.9
T5	-2.2	10.9	11.2
CB3	-4.7	16.1	2.4
GS3	-3.4	12.7	5.9
GL3	-4.3	13.0	3.6

Table 4: Mass and volume changes caused by heat-treating samples at 1 500 °C together with measured cold crushing strengths of the fired castables.

	Δm [%]	ΔV [%]	CCS [MPa]
X	-1.6	18.9	24.5
T1	-1.6	11.7	35.1
T2	-1.8	6.3	38.1
T3	-1.6	-1.4	42.4
T5	-1.8	-2.0	50.3
CB3	-4.2	14.0	14.2
GS3	-3.7	19.2	24.7
GL3	-4.4	18.2	15.7

For the graphite-containing samples GS3 and GL3, no crack formation was observed. However, for the heat-treated samples GL3, the mechanical strength also proved to be substantially lower than that of the reference samples (Tables 3 and 4). SEM investigations on samples fired at 1 500 °C revealed that sample GL3 is more porous than sample GS3 and CB3 (Fig. 2). The formation of larger pores in sample GL3 is probably a direct result of the use of large-flake graphite, which might provoke by combustion the formation of larger pores than small-flake graphite. In general, carbon sources with a larger grain size do effect a more uneven distribution of the carbon in the microstructure [18]. It has been shown that the adhesive force between two platelets increases with the size of their contact area [19].

Consequently, the larger graphite flakes should also possess a higher affinity to form building blocks by stacking. Combustion of locally accumulated carbon could thus account for an increased average pore size in the heat-treated sample GL3 compared to both the reference sample X and the carbon-containing samples CB3 and GS3.

Table 5: Phase compositions of samples heat-treated at 1 200 °C, values in wt%.

	Spinel	Corundum	β-Alumina	Periclase	Rutile	Garnet	Others
X	46.9	33.9	0.9	18.2	-	-	0.1
T1	54.1	29.5	0.9	15.0	-	-	0.5
T2	55.9	28.1	0.9	14.5	0.2	0.3	0.1
T3	57.4	27.9	0.9	12.9	0.3	0.3	0.3
T5	61.3	23.2	0.7	12.7	0.3	0.3	1.5*
CB3	51.4	31.3	0.8	16.5	-	-	0.0
GS3	48.0	33.1	0.7	18.2	-	-	0.0
GL3	38.4	39.2	1.0	21.4	-	-	0.0

* Sample T5: 1.1% olivine

Table 6: Phase compositions of samples heat-treated at 1 500 °C, values in wt%.

	Spinel	Corundum	β-Alumina	β-Alumina, Mg-rich	Periclase	Perovskite	Others
X	91.6	3.3	0.6	0.6	3.5	0.0	0.4
T1	96.7	1.2	0.6	0.4	0.9	0.0	0.2
T2	98.7	0.4	0.0	0.0	0.1	0.1	0.7
T3	98.4	0.2	0.0	0.0	0.0	0.4	1.0*
T5	96.3	0.1	0.0	0.0	0.0	0.4	3.0$
CB3	92.1	2.8	0.5	0.5	3.7	-	0.9
GS3	92.2	3.3	0.4	0.2	3.4	-	0.7
GL3	91.8	3.4	0.4	0.5	3.8	-	0.6

* Sample T3: 0.7 wt% karrooite
$ Sample T5: 3 wt% karrooite

IV. Conclusions

Small additions of titania added in a magnesia alumina castable were found to exert a large influence on the *in-situ* spinel formation at elevated temperatures. Investigations on the microstructure of the fired refractory suggest that titania additions promote the grain sintering of spinel in favor of grain growth by Ostwald ripening. Furthermore, the improved sinterability diminished the volume expansion associated with the spinelization in the castable and increased the cold crushing strength of the heat-treated castables. The titania additions were also found to increase the amount of spinel developing during heating. For castables containing titania in amounts from 0 to 5 wt%, heat treatment at 1 200 °C resulted in the formation of spinel in amounts of 46.9 to 61.3 wt%.

Compared to the spinel content in additive-free reference samples, the addition of 3 wt% of carbon black or small-flake graphite effected a slight increase of the amount of *in-situ*-formed spinel when the castables were fired at 1 200 °C. Through the addition of large-flake graphite, however, a significantly smaller amount of spinel crystallized at this temperature. This effect was attributed to separation of magnesia and alumina grains by layers of large-graphite flakes preventing the progress of the spinelization.

References

1 Kim, T., Kim, D., Kang, S.: Effect of additives on the sintering of $MgAl_2O_4$, *J. Alloy. Compd.*, **587**, 594 – 599, (2014).

2 Mohan, S.K., Sarkar, R.: A comparative study on the effect of different additives on the formation and densification of magnesium aluminate spinel, *Ceram. Int.*, **42**, 13932 – 13943, (2016).

3 Mohan, S.K., Sarkar, R.: Effect of ZrO_2 addition on $MgAl_2O_4$ spinel from commercial grade oxide reactants, *Ceram. Int.*, **42**, 10355 – 10365, (2016).

4 Kusiorowski, R.: Effect of titanium oxide addition on magnesia refractories, *J. Aust. Ceram. Soc.*, **56**, 1583 – 1593, (2020).

5 Angelkort, J., Cichocki, M., Higgins, S., Lakotta-Weinhold, Y., Fröse, N., Mix, M.: The in-situ spinel formation in a magnesia alumina castable and the effect of selected additives on the properties of the castable, *Open Ceram.*, **16**, 100503, (2023).

6 Braulio, M.A., Rigaud, M., Buhr, A., Parr, C., Pandolfelli, V.C.: Spinel-containing alumina-based refractory castables, *Ceram. Int.*, **37**, 1705 – 1724, (2011).

7 Nakajima, H.: The discovery and acceptance of the kirkendall Effect: the result of a short research career, *JOM*, **49**, 15 – 19, (1997).

8 German, R.M., Suri, P., Park, S.J.: Review: liquid phase sintering, *J. Mater. Sci.*, **44**, 1 – 39, (2009).

9 Yang, H., Hazen, R.M.: Comparative high-pressure crystal chemistry of karrooite, $MgTi_2O_5$, with different ordering states, *Am. Mineral.*, **84**, 130 – 137, (1999).

10 Kornaus, K., Czekaj, I., Sobuś, N., Lach, R., Gubernat, A.: Remarkable structural modifications of tialite solid solutions obtained by different methods, *Materials*, **15**, 3981, (2022)

11 Cao, R., Ye, H., Li, H., Schulze-Bergkamen, H., Zhang, H.: Preparation and properties of fiber/whisker composite magnesia-alumina spinel refractory by in-situ chemical vapor deposition. In: Proceedings of the 18th Unified International Technical Conference on Refractories, UNITECR 2023, Frankfurt/Main, Germany, 2023.

12 Naghizadeh, R., Zezaie, H.R., Golestani-Fard F.: Effect of antioxidants and atmosphere on the phase formation and microstructure of in situ MgO-Al_2O_3 spinels, *Defect Diffus. Forum*, **273 – 276**, 542 – 548, (2008).

13 Raj, S.S., Gupta, S.K., Grover, V., Muthe, K.P., Natarajan, V., Tyagi, A.K.: $MgAl_2O_4$ spinel: synthesis, carbon incorporation and defect-induced luminescence, *J. Mol. Struct.*, **1089**, 81 – 85, (2015).

14 Gražulis, S., Daškevič, A., Merkys, A., Chateigner, D., Lutterotti, L., Quirós, M., Serebryanaya, N.R., Moeck, P., Downs, R.T., LeBail, A.: Crystallography Open Database (COD): An

open-access collection of crystal structures and platform for world-wide collaboration, Nucleic Acids Res., 40, D420 – D427, (2012).

[15] Zhou, H., Sun, W., Huang, J., Wang, K., Chen, X., Liu, X., Ruan, H.: Crystal structure, microstructure and microwave dielectric properties of novel $MgAl_2Ti_3O_{10}$ ceramic, *J. Mater. Sci.*, **29**, 6232 – 6235, (2018).

[16] Shon, I-J., Kang H-S., Doh, J-M., Yoon, J-K.: Rapid synthesis and consolidation of nanostructured $2MgAl_2O_4$-$MgAl_2Ti_3O_{10}$ composite and its mechanical properties, *Res. Chem. Intermed.*, **40**, 2407 – 2413, (2012).

[17] Suzuki, Y., Shinoda, Y.: Magnesium dititanate (MgTi2O5) with pseudobrookite structure: a review, *Sci. Technol. Adv. Mater.*, **12**, 034301, (2011).

[18] Li, S., Liu, J., Wang, J., Zhu, Q., Zhao, X., Zhang, H., Zhang, S.: Fabrication of graphitic carbon spheres and their application in Al_2O_3-SiC-C refractory castables, *Int. J. Appl. Ceram. Technol.*, **15**, 1166 – 1181, (2018).

[19] Gu, Z., Li, S., Zhang, F., Wang, S.: Understanding surface adhesion in Nature: A peeling model, *Adv. Sci.*, **3**; 1500327, (2016).